Vol. 12(3), pp. 87-106, July-September, 2020
DOI: 10.5897/JGMR2020.0331
Article Number: 9D786DB64793
ISSN 2006-9766

http://www.academicjournals.org/JGMR

ACADEMIC JOURNALS
expand your knowledge

Journal of Geology and Mining Research

Full Length Research Paper

LA-ICP-MS and EMP relationships in pyrite grains from Barberton Greenstone Belt, South Africa: An attempt for quantification

Mohammed Alnagashi Hassan Altigani

Department of Geology of Minerals Wealth, Faculty of Petroleum and Minerals, Alneelain University, Khartoum, Sudan.

Received 28 January, 2020; Accepted 15 May, 2020

Laser Ablation Inductively Coupled Plasma Mass Spectrometry (LA-ICP-MS) count per seconds (cps) results were tested for quantification, using the same spot analyses of Electron Microprobe Analyses (EMP) in weight percentage (wt. %); they were obtained from selected pyrite grains from Sheba, New Consort, and Fairview gold mines of the Barberton Greenstone Belt (BGB). Theoretically, data obtained from the same pyrite grains, using two different techniques must represent, to some extent, the same chemical composition, but not exclusively the same values. This comes because they applied to the same spots, and within the same pyrite grains. Yet, the results obtained in this study of the two techniques are not directly comparable. Graphical and statistical techniques were also applied to depict any existing relationships. However, all do not indicate any kind of similarity in the distribution of major or trace-elements in the pyrite of both datasets. The results of this study imply that the obvious correlations between data of the two techniques for matching spots are failed by several factors (spot size, zoning, heterogeneity, etc.), which are negatively influencing any direct standardization procedure of LA-ICP-MS data based on EMP results.

Key words: Laser Ablation Inductively Coupled Plasma Mass Spectrometry (LA-ICP-MS), electron microprobe, Barberton greenstone belt, pyrite, standardization.

INTRODUCTION

Due to its high range of sensitivity, high precision, low detection limits, and relatively large analysed sample volume, Laser Ablation Inductively Coupled Plasma Mass Spectrometry (LA-ICP-MS) is favoured over electron microprobe (EMP) analysis in many geological studies including ore minerals' identification (Sylvester et al., 2005; Humayun et al., 2010; Shaheen et al., 2012). In comparison, during EMP analysis mainly the surface of samples is examined.

The LA-ICP-MS technique requires minimal sample preparations (Shaheen et al., 2012) and the sample is directly analysed by spot ablation with a pulsed laser beam. The created aerosols are transported into the core of inductively coupled argon plasma (ICP) at a temperature of approximately 8000°C (Thomas, 2004). The plasma is used to generate ions, which are introduced to the mass analyser. The ions are separated and collected according to their mass values and charge ratios. The LA-ICP-MS has a higher sensitivity than the EMP and is probably able to detect concentrations below

E-mail: m.alnagashi@gmail.com. Tel: +249900090088.

1 part in 10^{12} (part per trillion) (Sylvester, 2008).

Study aim

This study aims to detect and evaluate the possible relationships between LA-ICP-MS and EMP results that were obtained from the same spots on the same selected pyrite grains. The concept of this paper was to use EMP results as standard match for standard-less LA-ICP-MS, which constructed on the hypothesis suggests analytical techniques must provide the same element compositions with possible differences in the quantities due to detection limits and/or spot size, etc. LA-ICP-MS data are reported as count per second (cps). The use of EMP analysed grains as matrix match for LA-ICP-MS assumes that ablation in the same spots within the selected pyrite grains are consistent and should result in a linear relationship between cps (LA-ICP-MS) and wt.% (EMP) for major and trace elements. In this research contribution, a standardization of the LA-ICP-MS by EMP was planned by analysing the same spots in selected pyrite grains from three mines (Sheba, Fairview, and New Consort), located in part of the Barberton Greenstone Belt (BGB) with both techniques (Table 1).

MATERIALS AND METHODS

In order to assess the variability of mineral compositions, the major and trace elements were measured using a *CAMECA SX-100* electron microprobe (University of Pretoria) and Laser Ablation Inductively Coupled Plasma Mass Spectrometry '*ICP-MS 7500 Series'* (Forensic Science Laboratory, Pretoria), respectively. The measurements were performed on epoxy mounted polished sections. The selected samples were prepared and analysed for major and trace element composition by electron microprobe at the University of Pretoria. The same samples (same spots) were subsequently analysed by laser ablation at the South Africa Police Forensic Laboratory in Pretoria.

Electron microprobe (EMP)

Imaging and elemental analysis were performed using an electron microprobe in the gold and sulphide ores from the Sheba, the Fairview, and the New Consort Mines. The spectra were processed by ZAF corrections. Analysis of the samples was performed with an accelerating voltage of 20 kV, a current of 20 nano-Ampere (nA), and a focused spot (1 µm diameter). Counting times were 10 s for all elements. The standards used for calibration were as follows: albite (Si, Na, K), MgO (Mg), Al_2O_3 (Al), topaz (F), apatite (P), andradite (Ca), orthoclase (K), Fe_2O_3(Fe), vanadinite (Cl) and MnTi standard (Mn, Ti).

Laser ablation inductively coupled plasma mass spectrometry (LA-ICP-MS)

Pyrite grains were analysed by LA-ICP-MS in order to determine elemental distribution within the grains. The trace elements were measured using an "*Agilent 7500 CX"* inductively coupled plasma mass spectrometer coupled to a *New Wave213* nm laser ablation was performed in He, and the gas then mixed with argon prior to delivery to the MS. Between run normalization was achieved using the bracketing technique over an NIST 612 glass analysed every 20 spots. For spot analyses, the samples were ablated using a spot size and depth of 25 µm, with an energy of 5 J/cm^2 and a 4 Hz repetition rate, for 45 s. The resolution of the laser spot is not as small as that, which is achievable by an electron microprobe, but elemental concentrations of a wide range of elements down to ppb levels are possible. The LA-ICP-MS results are not quantified to standards, but expressed as count per seconds (cps). A laser spot size of 10 µm was selected, with a scan speed of10 µms−1 and a sampling rate of ~0.25 s. This translates to an effective sampling area of 2.5 × 10 µm.

In this research, an Agilent Technologies model '*ICP-MS 7500 Series'* instrument was used at the South African Police Forensic Science Laboratory, Pretoria, South Africa. This machine is equipped with a high-performance "*NEW WAVE model UP-213"* laser ablation system. This system is presently considered the best type to reduce and minimize the inter-elemental fractionation that could be caused by local temperature changes, ablation time, and variations in the matrix matched elements (Chen, 1999; Gaboardi and Humayun, 2009, Woodhead et al., 2009). The fluency value of the laser beam is > 30 J/cm^2.

The samples were placed in the ablation cell, and the aerosol produced by ablation is swept into the mass spectrometer using a stream of ultrahigh purity He gas (800 ml/min). A stream of Argon gas with flow rate of 900-1400 ml /min was added downstream to achieve the differential flow needed to obtain a bright, stable signal. A CCD (charge-coupled device) camera allows imaging of the sample during ablation. The operating *MEOLaser 213* software was used to analyze the trace elements in the sulphides and gold of the New Consort, the Sheba, and the Fairview mines of the BGB. The radio frequency (RF) power was 1200 Watt, and the carrier gas, (optional gas 95%, 0.90-0.95 L/min). The laser ablation power was 50% with 15 s delay time; the consistent spot size and depth was 25 µm with 10 Hz pulse repetition rate and 100% power output. The spots were each ablated for 45 s to reduce the possible inter-elemental fractionation. The machine performance of the LA-ICP-MS was calibrated with international standards as mentioned in Sylvester (2008). The operational parameters were optimized using argon (Ar) gas blanks, and NIST glasses 610 and 612 before analysing an individual mineral grain. The procedure was also repeatedly applied during large numbers of analyses in large grains. The selection of these materials instead of pure gold and sulphide standards is due to the optimization requires a creation of a steady state signals, and continuous ablation of gold and sulphides may result in coating the core of the laser cell, which contaminates the system for a significant time (Watling and Herbert, 1994). The use of NIST glasses is applicable and suitable for measuring reproducibility and instrumental optimization (Watling and Herbert, 1994). Sylvester (2008) suggested that NIST 610 glass might be used to measure concentrations of Cu, Zn, Ag, Pt, and Au in sulphides with an accuracy of 10% using Fe as internal standard. However, this line of analysis is not approached due to the effects of small amounts of impurities in the pyrite, which disturb the ablation rates even if same matrixes are used. After analyses, the raw data were cleaned from the background noise by subtracting the blank count per second values from the data for the same spots. The first 50 analyses were omitted from the data set to avoid the background noise. Glass, gold and sulphides are not the same material. That means the plasma loading will vary between the three materials; the technique used in this research was not based on the quantification or absolute values of the analysed elements, but on their counts per second. Once the calibration had been accomplished, reference blanks were also analysed using the same analytical conditions, and then subtracted from the results. As LA-ICP-MS technique used in this study is a standard less technique, it is highly recommended to verify comparability of the element associations in the samples with data from previous analyses at the same areas (Watling and Same, 1994).

Table 1. The standardization of LA-ICP-MS (cps) results of Sheba Mine to their S, Fe, and the sum of all counts. Also shown the EMP (wt. %) results for the same analysed spots on selected pyrite grains.

Mine	$^{33+34}$S	S normalized to sum	S normalized to Fe	$^{56+57}$Fe	$Fe_{(t)}$ normalized to sum	Fe normalized to $S_{(t)}$	^{59}Co	^{59}Co normalized to Sum	^{59}Co normalized to sulphur	^{59}Co normalized to $Fe_{(t)}$	^{60}Ni	^{60}Ni normalized to sum
Sheba	1220320	441035	6931	176067274	99190435	1442796125	436 22	15740	357465	248	37236	13436
Sheba	1134078	440695	7229	156871674	99196799	1383253143	0	0	0	0	36201	14042
Sheba	1187293	429075	6740	176150874	99278191	1483634474	0	0	0	0	15583	5623
Sheba	1333772	483927	7628	174840898	98990346	1310875219	0	0	0	0	27463	9947
Sheba	1217285	441927	6967	174725501	99052093	1435370240	0	0	0	0	118627	42998
Sheba	479615	242039	4886	98163862	99313808	2046720602	1087	548	22662	11	2074	1045
Sheba	520135	232297	4203	123763561	99406350	2379451055	890	397	17114	7	2944	1314

Mine	^{60}Ni normalized to $S_{(t)}$	^{60}Ni normalized to $Fe_{(t)}$	^{75}As	^{75}As normalized to Sum	^{75}As normalized to $S_{(t)}$	^{75}As normalized to $Fe_{(t)}$	Total of cps	S wt%	Fe wt%	As wt%	Co wt%	Ni wt%
Sheba	305132	211	135 835	49012	1113111	771	1720631046	52.83	46.2	1.2	0.01	0.4
Sheba	319208	231	999 18	38757	881052	637	1641373218	52.73	46.3	0.8	0.2	0.3
Sheba	131247	88	778 42	28087	655624	442	1760917030	52.46	46	0.6	0	0.7
Sheba	205906	157	422 058	152860	3164395	2414	1587197321	52.63	45.6	1.2	0	0.8
Sheba	974521	679	336 173	121831	2761658	1924	1712287010	52.4	45.8	1.1	0.1	0.5
Sheba	43242	21	195 470	98524	4075566	1991	2245190973	52.17	46.3	0.3	0	0
Sheba	56605	24	215 140	95983	4136242	1738	2603672037	52.22	46.2	0.6	0	0.1

RESULTS

Relationship between EMP and LA-ICP-MS

The raw LA-ICP-MS data (cps) of S, Fe, As, and Ni were plotted versus EMP data (wt.%) before any standardization to detect any possible relationship (Figure 1). Cobalt was omitted from the evaluation because most of EMP and LA-ICP-MS results are below the detection limits. The figure shows that there is no direct relationship between the two measuring techniques. Based on their Ni content, Figure 1A suggests two groups of pyrite in the Fairview Mine. In comparison, the New Consort Mine pyrite grains show elevated Ni values.

Iron seems to be more consistent in all three mines (Figure 1B). However, the overall correlation does not show any positive relationship between EMP and LA-ICP-MS results for the selected pyrite grains. Figure 1C illustrates that sulphur values (in cps) for the New Consort Mine are very low compared to the other mines. Arsenic contents in the Fairview Mine pyrite have the highest values between all mines (Figure 1D).

Normalizing the LA-ICP-MS to their summation

The ablation rate of major elements (S, Fe) and trace elements (As, Ni, Co) of pyrite fluctuated during the LA-ICP-MS analyses. In order to avoid any unpredictable fluctuation in ablation rate due to intrinsic differences between pyrite grains, the data for each analysis were summed up, and normalized to the sum of all reported isotopes (Table 1). In this way, analytical errors, which could be caused by lower detection limits and the heterogeneous nature of analysed grains (Ciobanu et al., 2009), and inter-element fractionation, which might result from non-stoichiometric sampling during the ablation process, or incomplete vaporization of large particles (inclusions >125 nm) in the plasma, should be compensated for (Gaboardi and

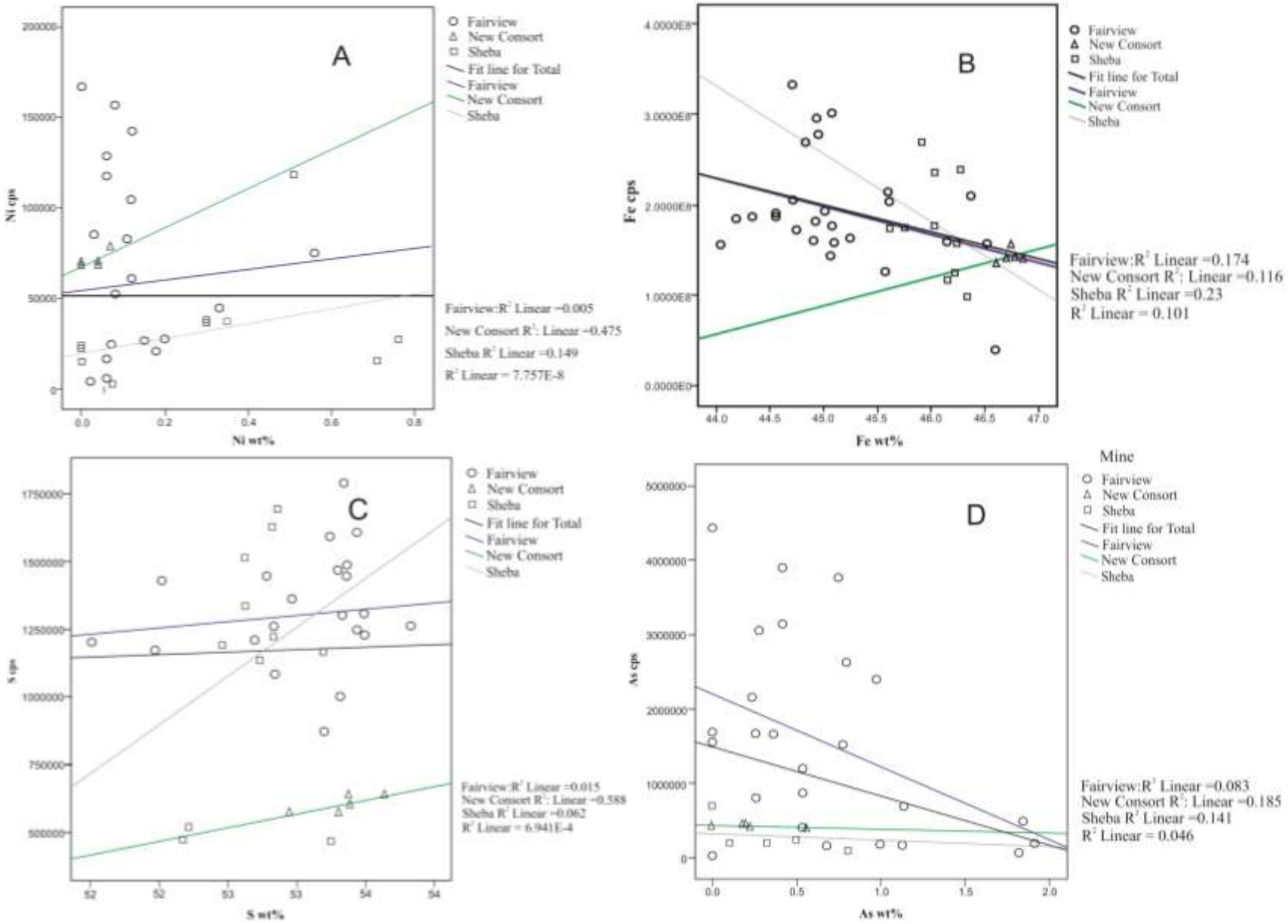

Figure 1A, B, C, and D. Correlation between EMP and raw LA-ICP-MS results in pyrite from Sheba, New Consort, and Fairview mines. n for Sheba: 11, for Fairview: 26, and for New Consort: 5.

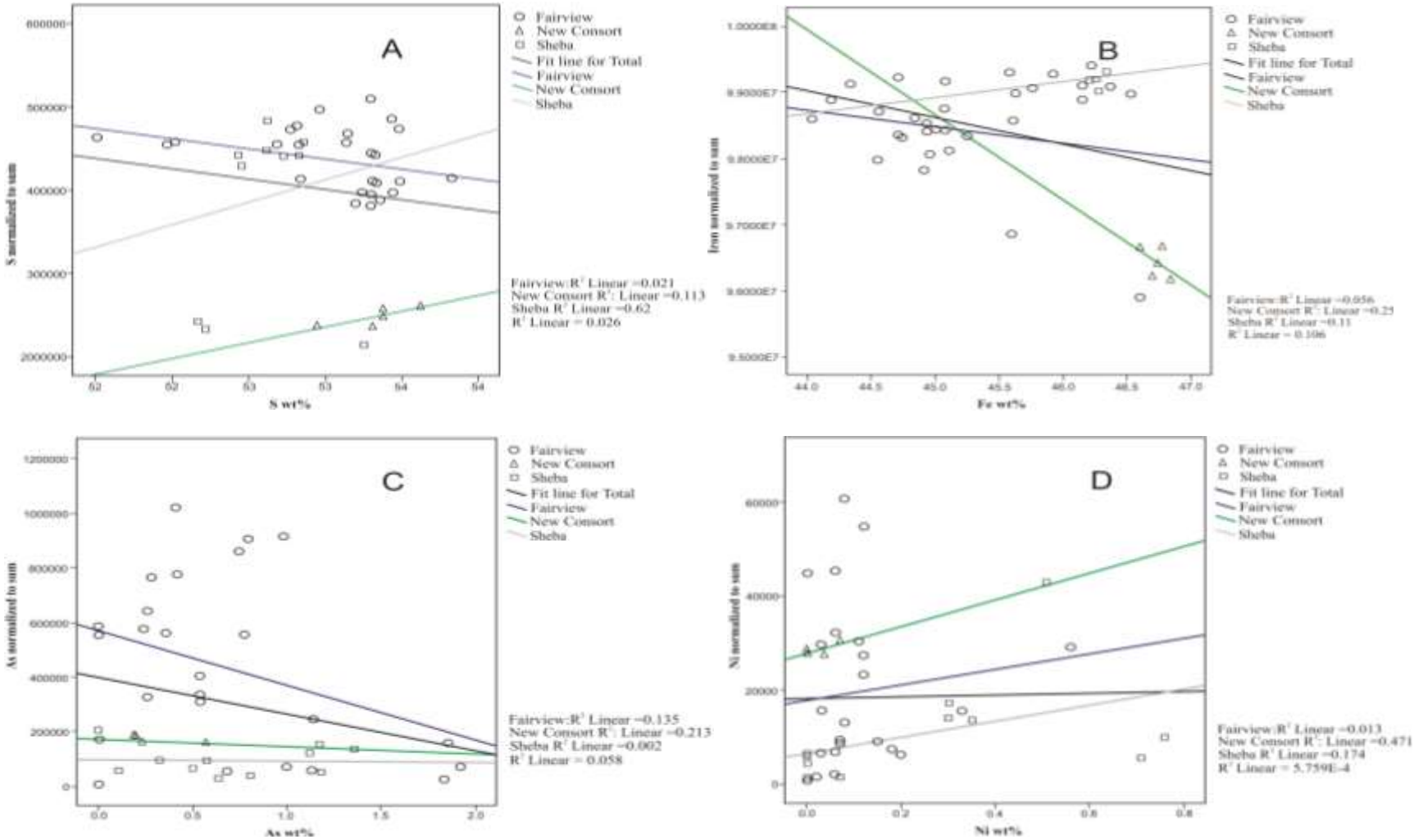

Figure 2A, B, C, and D. Correlation between EMP & normalized (Fe, S, Ni, & As) to their SUM in pyrite from three mines. n for Sheba: 11, for Fairview: 26, and for New Consort: 5.

Humayun, 2009).

The normalized results were plotted versus the EMP data of the same spots for the elements [33, 34]S, [75]As, [56, 57]Fe, and [60]Ni (Figure 2). No positive trends or relationship between the two datasets were noticed. Figure (2A) confirms the low sulphur values observed in pyrite of the New Consort Mine (as shown in Figure (1A). The iron content is low as well in pyrite of the New Consort correlated to the Sheba and Fairview mines (Figure 2B). Figure 2C displays that (As) could be used to classify the pyrite of the Fairview Mine into two

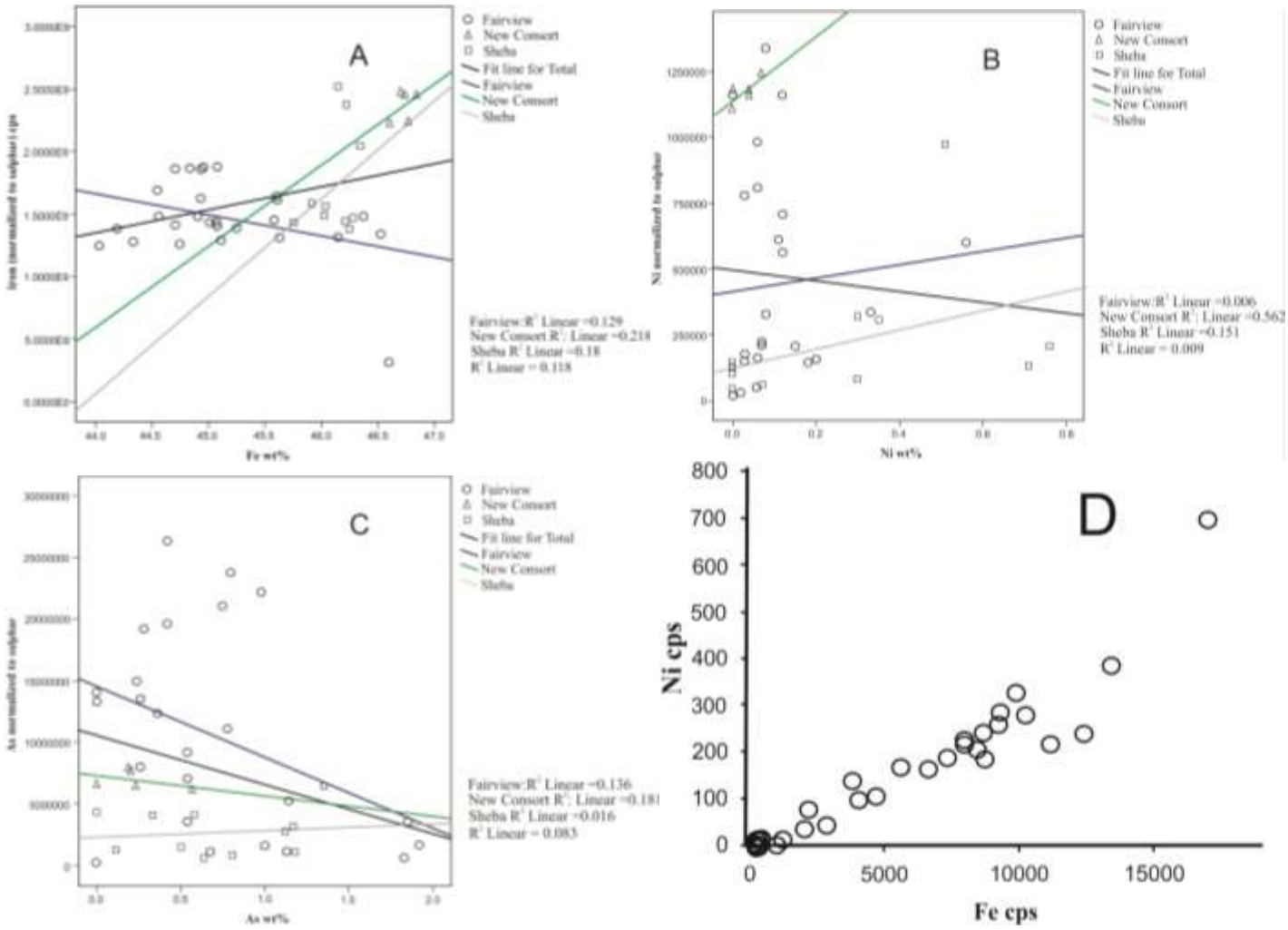

Figure 3A, B, C. Normalization of Fe, As, and Ni to the sulphur contents in pyrite from the three mines. **D)** reflects inconsistent relationship between Fe and Ni in pyrite grains from the Sheba Mine. n for Sheba: 11, for Fairview: 26, and for New Consort: 5.

groups, while its concentrations in both Sheba and New Consort mines are relatively homogenous. Nickel (Figure 2D) does not reflect any kind of relationships. Although problems due to ablation rate variability could possibly be eliminated by normalization, no systematic or positive relationships between EMP and LA-ICP-MS could be confirmed.

Using sulphur as internal standard

The LA-ICP-MS results for Fe, Ni, and As were also normalized to the sulphur content, and then compared to their equivalent EMP data (Figure 3). Sulphur was used as internal standard, because of its fixed content in the pyrite lattice, which controls the pyrite lattice structure. Thus, less ablation variations were expected among the LA-ICP-MS data. Godel and Barnes (2008) used sulphur as internal standard for platinum group minerals (PGM) from the Bushveld Igneous Complex. Yuan et al. (2012) noted a reduction on the internal fractionation levels by using sulphur as internal standard; they used USGS poly-metal sulphide reference material MASS-1 as well as NIST for ICP machine calibration. They concluded that using sulphur as internal standard with NIST 612 is better than using iron as internal standard with NIST 612. Their method gave only 10% errors for the major elements, and reflect good results for elements like S, Co, Ni, Ag, and Au. However, Sylvester (2008) noticed the large interference (~40%) between oxygen and some of sulphur isotopes. Therefore, the author found it very difficult to exercise S isotopes as internal standard.

Figure (3A) demonstrates higher values of iron (in cps) in the New Consort Mine rather than the Sheba and Fairview mines, which is contradicted by the high Ni (cps) values as seen in Figure 3B. Arsenic (Figure 3C) as well as nickel varies significantly in pyrite of the Fairview Mine, which indicates two pyrite generations. Figures (3D) shows an uncommon relationship between Ni and Fe, which should not exist because of substitution

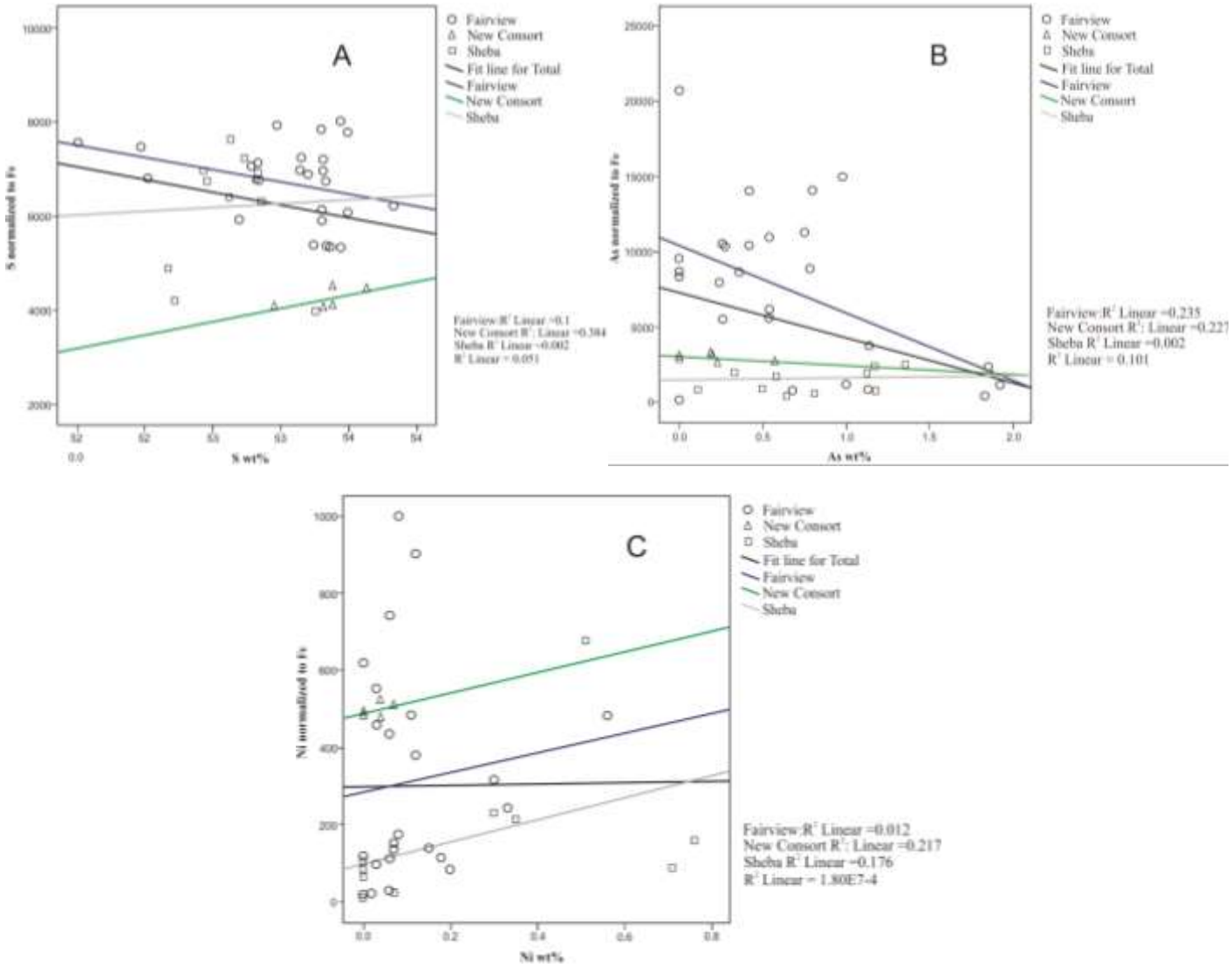

Figure 4A, B, and C. Normalization of S, As, and Ni to the iron contents in pyrite from the three mines. it also reflects the high Ni value in the pyrite of the New Consort Mine related to Sheba and Fairview. n for Sheba: 11, for Fairview: 26, and for New Consort: 5.

between the two elements.

Danyushevsky et al. (2011) introduced a new matrix matched standard named *STDGL2b2*, which is composed of powdered sulphides (pyrite, pyrrhotite, galena, sphalerite, and chalcopyrite), doped with certified element solutions, and fused to a lithium-borate glass disk. The standard is used for quantitative analysis of trace elements in a range of sulphide matrices (Bi et al., 2011; Danyushevsky et al., 2011; Cook et al., 2011). Analytical errors for Fe are <15% if used as external standard, but the authors conclude that Fe can be safely used as an internal standard. They argued that sulphur is not the suitable element to be utilized as internal matrix matched standard for the sulphides, due to its large remembrance effects within the LA-ICP-MS equipment regularly used for sulphides analyses, besides the high intensities of chemical interferences (e.g. $^{16}O_2$ on ^{32}S) (Danyushevsky et al., 2011).

The use of iron as internal standard

In order to reduce fluctuation effects coupled with the problems mentioned before caused by using sulphur as internal standard, iron was recommended by several studies to replace sulphur as internal standard (Cook et al., 2009a; Danyushevsky et al., 2011; Winderbaum et al., 2012). Li and Audétat (2012) used iron as internal standard for LA-ICP-MS analyses of upper mantle sulphides. In this study, iron was tested as internal standard as well. LA-ICP-MS results of some selected elements (S, As, Ni) were normalized to the Fe content, and then plotted against their equivalent EMP results.

Figure (4A) confirms the low values of sulphur in New

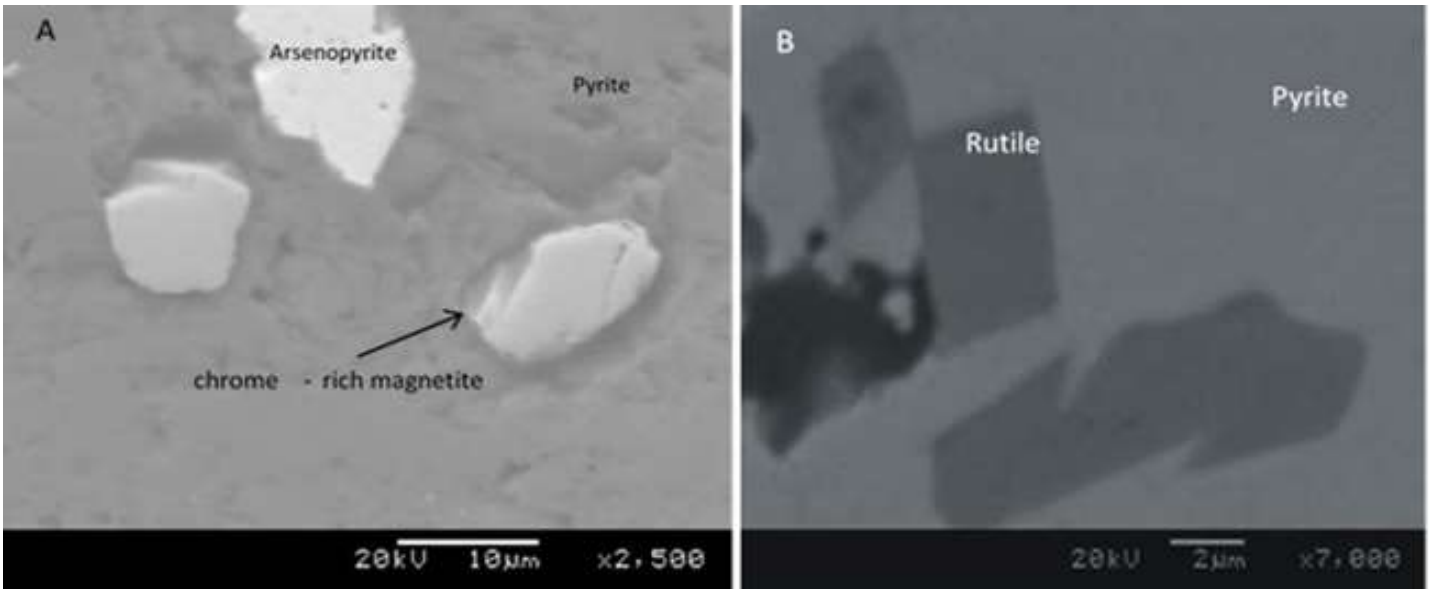

Figure 5. Back-scattered electron images of pyrite grain from the Fairview Mine, indicating micro-grains of (A) chrome-rich magnetite and (B) rutile within the pyrite.

Consort Mine pyrite, when normalizing the data to their summation, or sulphur contents. The As and Ni values of the New Consort Mine are high compared to the Sheba and Fairview mines (Figures 4B and C). These two elements (As and Ni) could also be used as classifying factor for pyrite of the Fairview Mine into two generations (types). No significant relationships between EMP and LA-ICP-MS were observed when using iron as internal standard.

The observed relationships of the elements using LA-ICP-MS results indicate possible links between differences in ablation rate and the chemical compositions of the analysed grains. Nickel values in the pyrite grains are significantly increased in the New Consort Mine, replacing iron in the pyrite. Fractionation between Fe and Ni may occur at the ablation spot, and can be influenced by enclosed tiny mineral domains in the selected pyrite (Figure 5A and B), or by the effects of laser parameters including wavelength, fluency and lateral energy distribution, pulse repetition rate, focal length of the objective lens, and focus position relative to the examined samples (Heinrich et al., 2003). Ni and Co (and to some extend arsenic) usually replace iron in pyrite. Consequently, a negative relationship between Fe and any of the substituting elements (Ni in particular) should exist. However, as revealed in Figure 3D, a positive relationship is implied by the LA-ICP-MS data. This deceptive contradiction cannot be an effect of actual mineral chemistry, but can possibly be related to effects of ablation rate as a function of mineral chemistry. Most of the chosen pyrite grains in this study reflect at least two different mineralisation events with significant variations in the trace elements contents (Altigani et al., 2016). So, as demonstrated in Figure 6, the ablation rate tends to be higher if the concentration of Ni is elevated in pyrite due to zoning or heterogeneity.

For the schematic evaluation shown in Figure 7, it was assumed that ^{60}Ni and (^{56}Fe+^{57}Fe) isotopes perform similarly during laser ablation due to close similarity in their atomic weights. Therefore, as more as pyrite is ablated during a laser shot, consequently more Ni will be detected as well. In addition, the effects of other inclusions and elements were ignored. The increase in Ni cps due to increase of ^{60}Ni contents in pyrite is relatively small compared to the overall increase in cps as result of higher ablation rate. Therefore, the positive trend observed in Figure 7 is mainly an effect of ablation rate differences as a function of pyrite characteristics. An increase in Ni has an effect on ablation rate, which exceeds the possible effects of substituting iron. The observed elemental relationships in the studied pyrite grains from the Fairview Mine show that the resultant LA-ICP-MS cps are indicative for the concentration, but do not define linear relationships. The elevated Ni contents in pyrite cause higher ablation rates. However, this may not be the only reason for an increase in the ablation rate. Furthermore, pyrite lattice defects, intergrowths between pyrite and marcasite domains, and the effects of other substituents may play a role. The presence of small inclusions (Figure 5), heterogeneities, and chemical zoning probably distorted the general relationships between the elements in the pyrite, as ablated volumes were large and deep, and hidden sub-surface domains or inclusions may chemically contribute to the results. Thus, removing these effects from the analyses is very important to achieve high precision for the pyrite analyses and elemental relationships in pyrite. Nevertheless, the inclusions and heterogeneities are very important

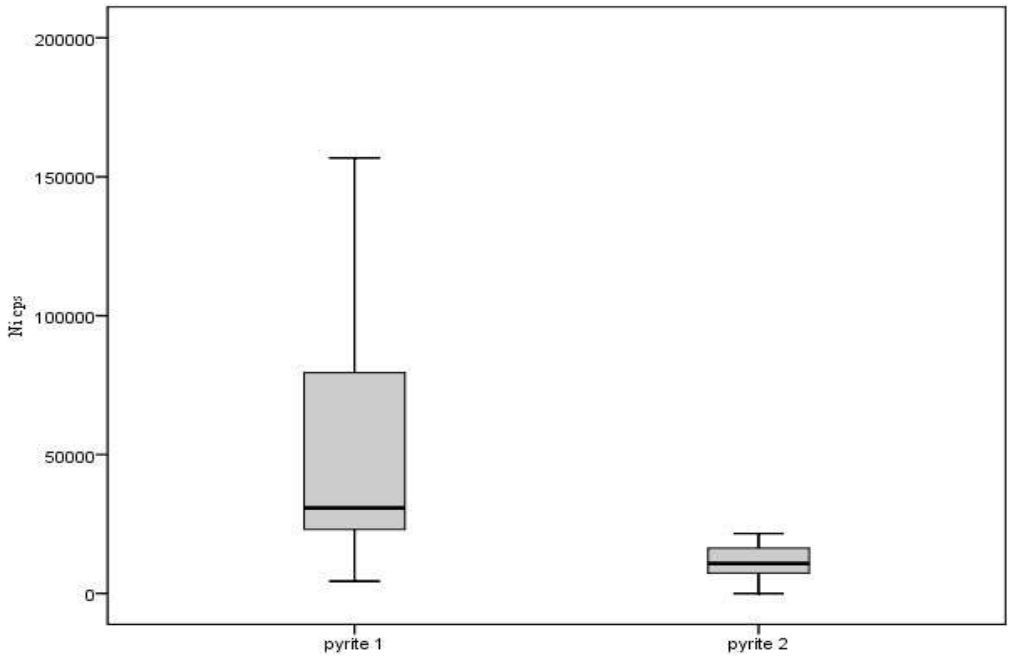

Figure 6. Shows higher Ni cps in pyrite type 1 compared to pyrite type 2 from the Fairview Mine. This implies differences in ablation rates between the two pyrite types. Based on the Ni and Fe relationship in pyrite obtained by EMP, Ni substitutes for Fe, and a negative relationship in cps should result.

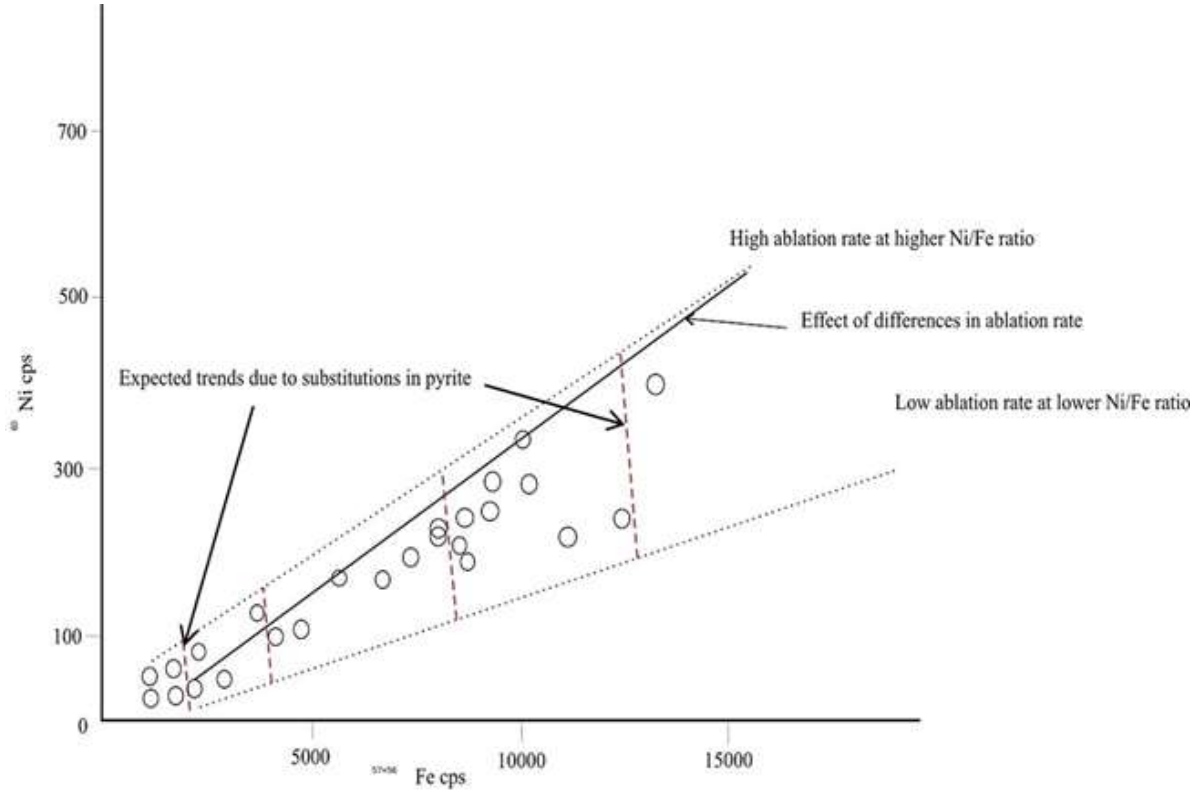

Figure 7. Assumed schematic relationship between Fe and Ni on the pyrite of the Fairview Mine. Due to the effects of ablation, the black (solid and dotted) trends were observed. The red dashed line represents the expected trends due to replacement between iron and nickel.

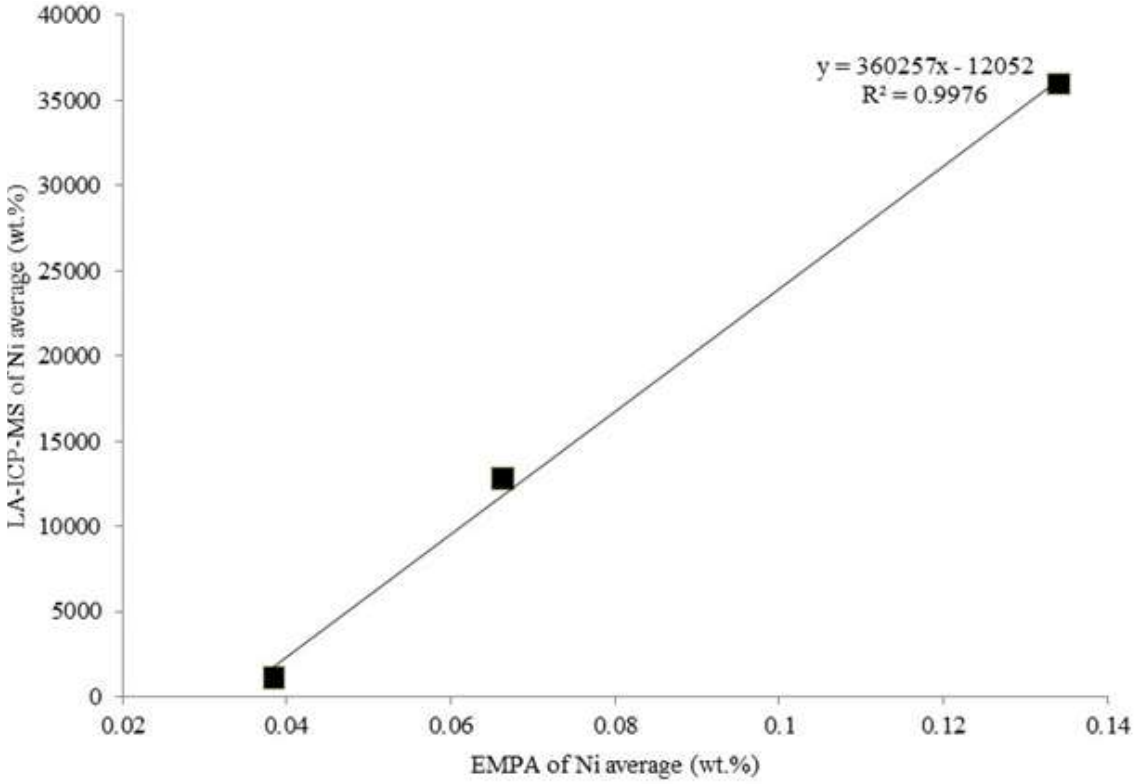

Figure 8. Comparison of average concentrations of Ni in pyrite type 2 of the Fairview Mine, obtained from the EMP (3 analyses per symbol) and with the LA-ICP-MS (3 analyses per symbol).

indicators for the formation history of pyrite.

Differences in result units

The results of the EMP are reported in weight present (wt. %), whereas the LA-ICP-MS results are described as count per seconds (cps), which directly reflects the elements detection (Oriano et al., 2008). The effects of all the difficulties mentioned above, together with the lack of exactly matrix matched material and standards for LA-ICP-MS, make it impossible to quantify the (cps) results with their equivalent EMP (wt.%) results.

In order to obtain a better understanding of the comparability of the results from the two techniques, it was decided to compare the arithmetic mean and standard deviation of the two datasets. Halter et al. (2004) noted a relationship between the calibration mean of LA-ICP-MS results of Fe, Co, Ni, and Cu that were obtained from pyrrhotite, chalcopyrite, and millerite grains with EMP results for the same elements and on the same spots. However, in this research, no systematic relationships were observed when means and standard deviations of LA-ICP-MS and EMP results for the elements S, Fe, Co, and As were compared. Incredibly, Ni is the only element that represents a positive correlation (Figure 8).

The arithmetic mean cannot be practiced as descriptive parameters for these data sets, since the datasets are not normally distributed. The normal distribution for the EMP and LA-ICP-MS results was tested using probability plot (P-P) technique (Figure 9 A_{1-4} and B_{1-4}). The regularity of the distribution for the EMP and LA-ICP-MS results was tested. It shows slight indication for normal distribution for both (Fe and Ni) values of EMP and LA-ICP-MS results; also it generally reflects that the distributions of both datasets at the same analysed spot are very similar, suggesting thought of well-matched distributions of both techniques can exist (Figure $9A_{1-4}$, and B_{1-4}).The compatibility between LA-ICP-MS and EMP data distributions, which observed from probability plot, indicates possible (uncertain) relationships between the two datasets. This implies that there are relationships, but it is not noticeable. This might refer to many factors, among others are: differences in ablation rate in the LA-ICP-MS, instrumental problems, and the variations of spot size and depths used in both techniques, and probably the sensitivity and limits of detection of the two techniques.

Box and whisker plots were used to depict any comparison between EMP and LAICP-MS results (Figure 10A and B). However, the boxplot does not indicate any

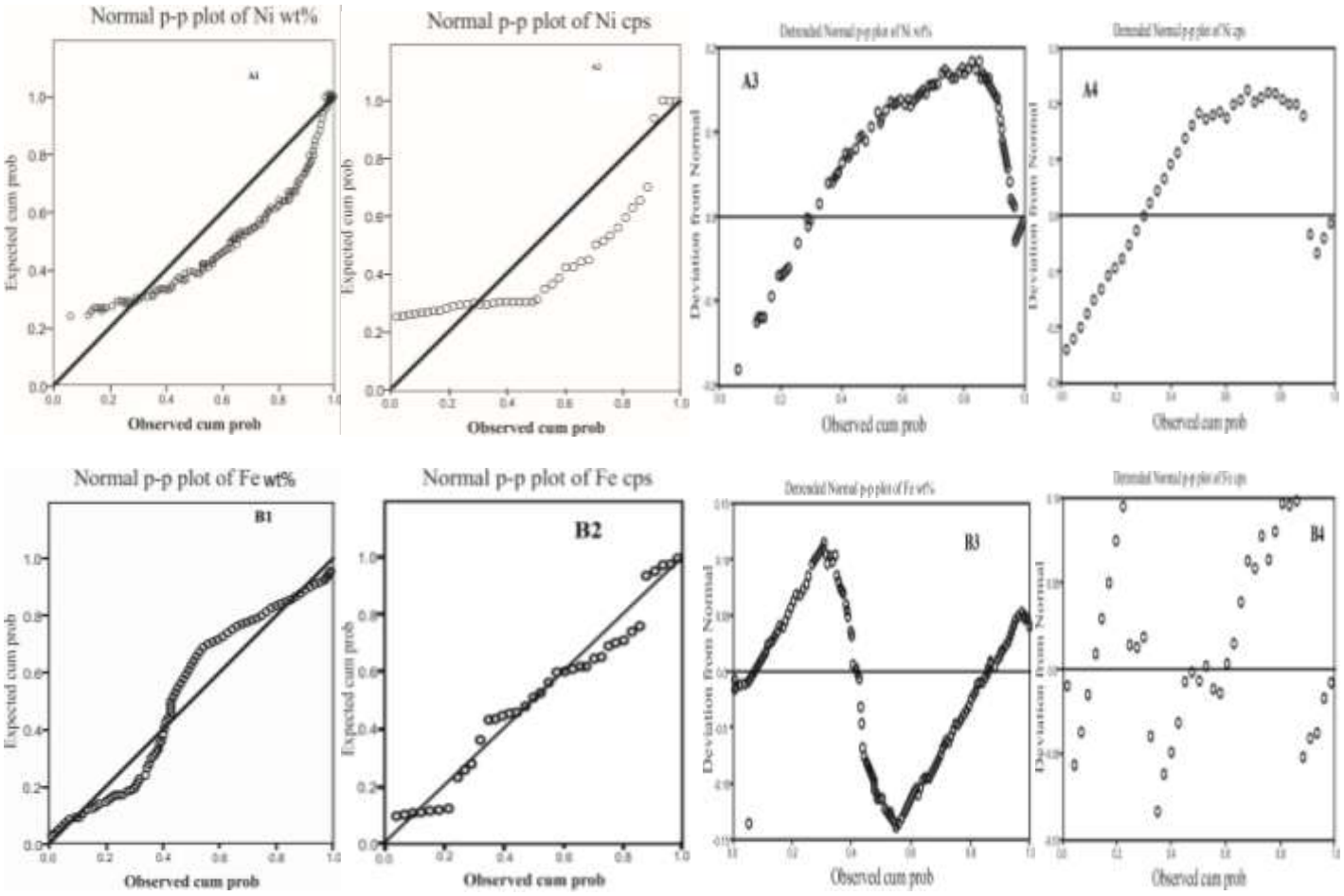

Figure 9. A1-4, B1-4. Probability plot (P-P) for iron and nickel selected pyrite grains from the Fairview Mine (A1-4): Ni wt.% compared to Ni cps, (B1-4): Fe wt. % compared to Fe cps.

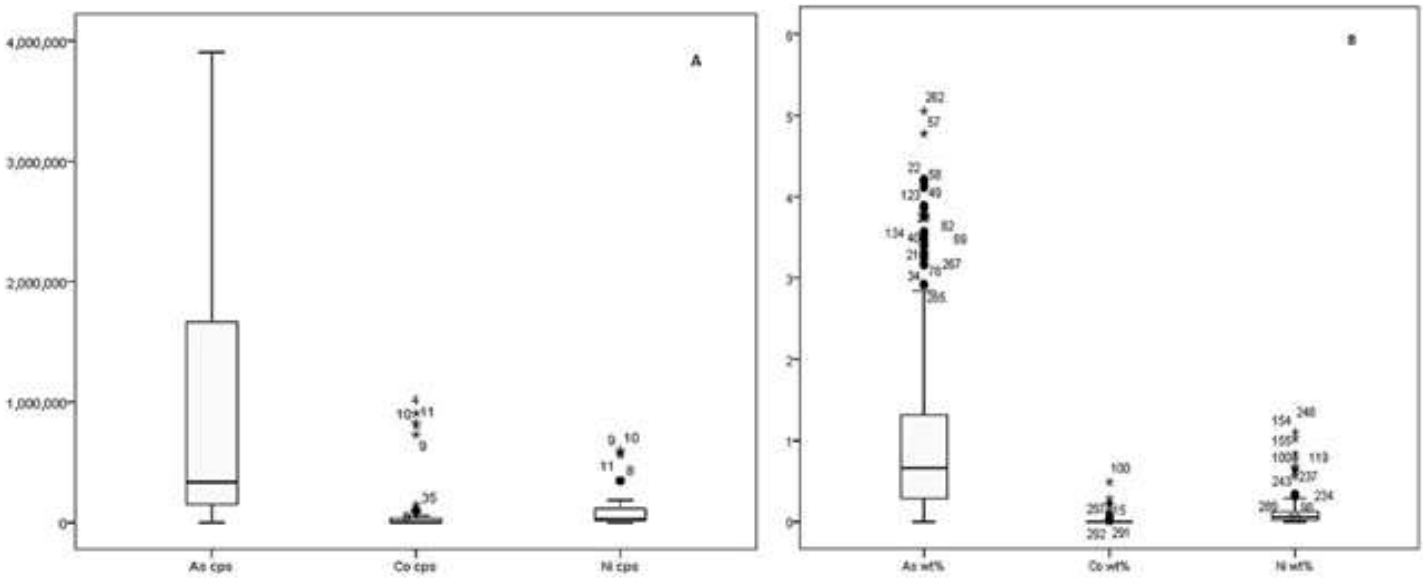

Figure 10. Box and whisker plots showing the skewed nature of the distributions of As, Co, and Ni in the pyrite type 2 from the Fairview Mine. A: LA-ICP-MS data, B: EMP data.

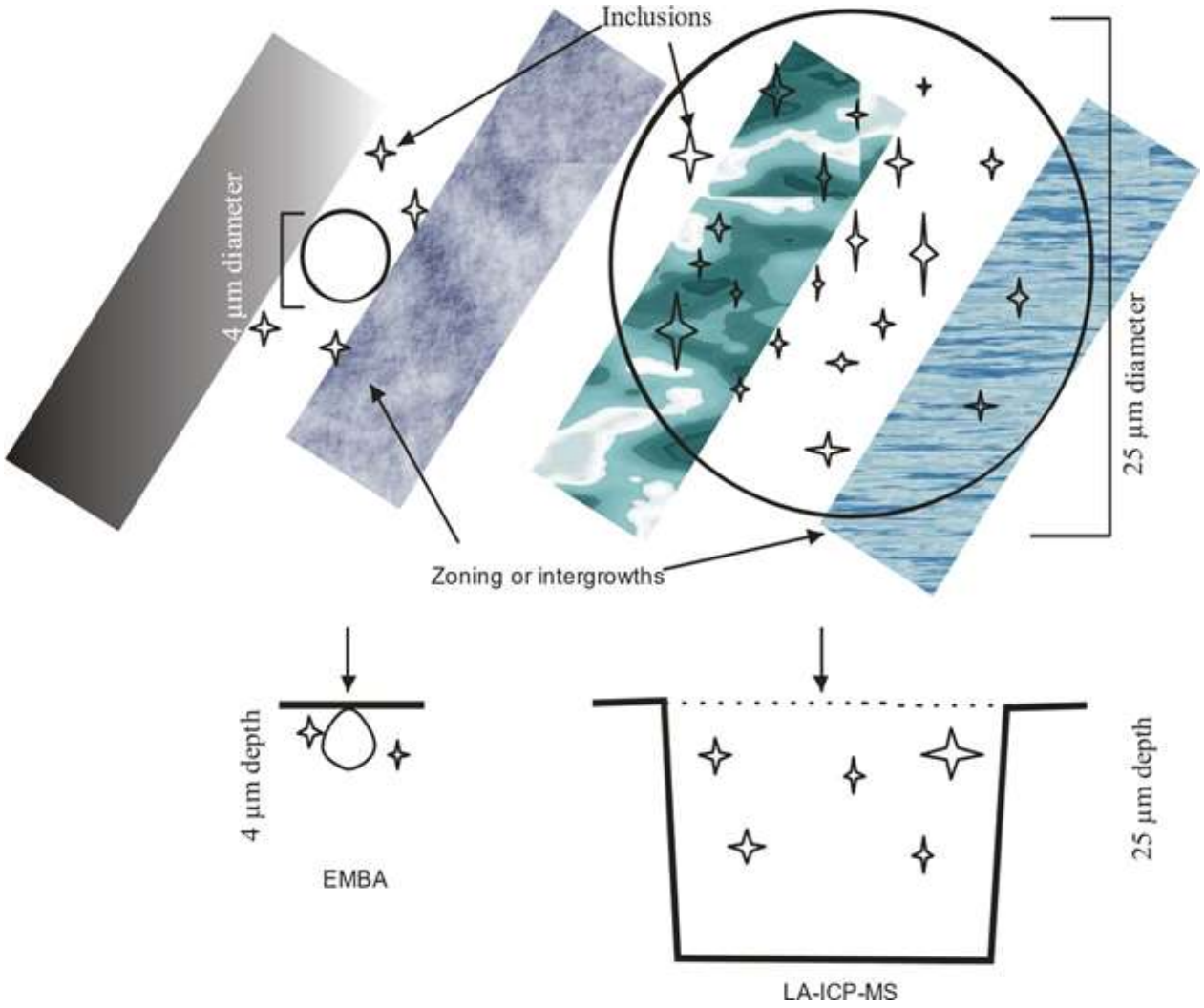

Figure 11. Schematic demonstration shows variations in spots size and depth between EMP and LA-ICP-MS methods.

kind of distribution similarity between the groups of elements (As, Co, and Ni) in both EMP and LA-ICP-MS. The LA-ICP-MS values (cps) are too high to present with the EMP results (wt. %) in same graph. Therefore, to make the data comparable in the scale, we assumed that the extreme values (high and low) in EMP results of a certain element are equal to the extreme values for the same element in LA-ICP-MS results. Consequently, the two techniques results were recalculated with the following formula:

Maximum value of EMP (in wt. %)=Maximum value of LA-ICP-MS (in cps) (1)

X (value of ICP wt. %) = the first EMP value of a certain element (2)

By matching (1) and (2) we can calculate the value of (x) as follows:

X (value of ICP wt. %) = Maximum value of EMP (wt.%) × the first EMP value for certain elements (wt.%) Maximum value of LA-ICP-MS (cps)

Despite that, no kind of relationships was observed except those of Ni (Figure 8). The variations between the spatial resolution (analysed spots size) of the LA-ICPMS (~25 µm) and EMP (~ 4 µm) cause differences in the chemical results of the examined pyrite grains (Figure 11A and B). Figure 12 A, B, and C shows that the cumulated frequency distributions (CFD) plot for EMP against LA-ICP-MS of the trace elements (Co, Ni, and As) are very similar. Despite that, sulphur and iron display larger deviation from the curve line (Figure 12D and E). This implies Co and Ni to a lesser degree are arsenic; analysing the same grains with both techniques will cause similar frequency distribution of the results, accordingly individual spots cannot be correlated. For Fe

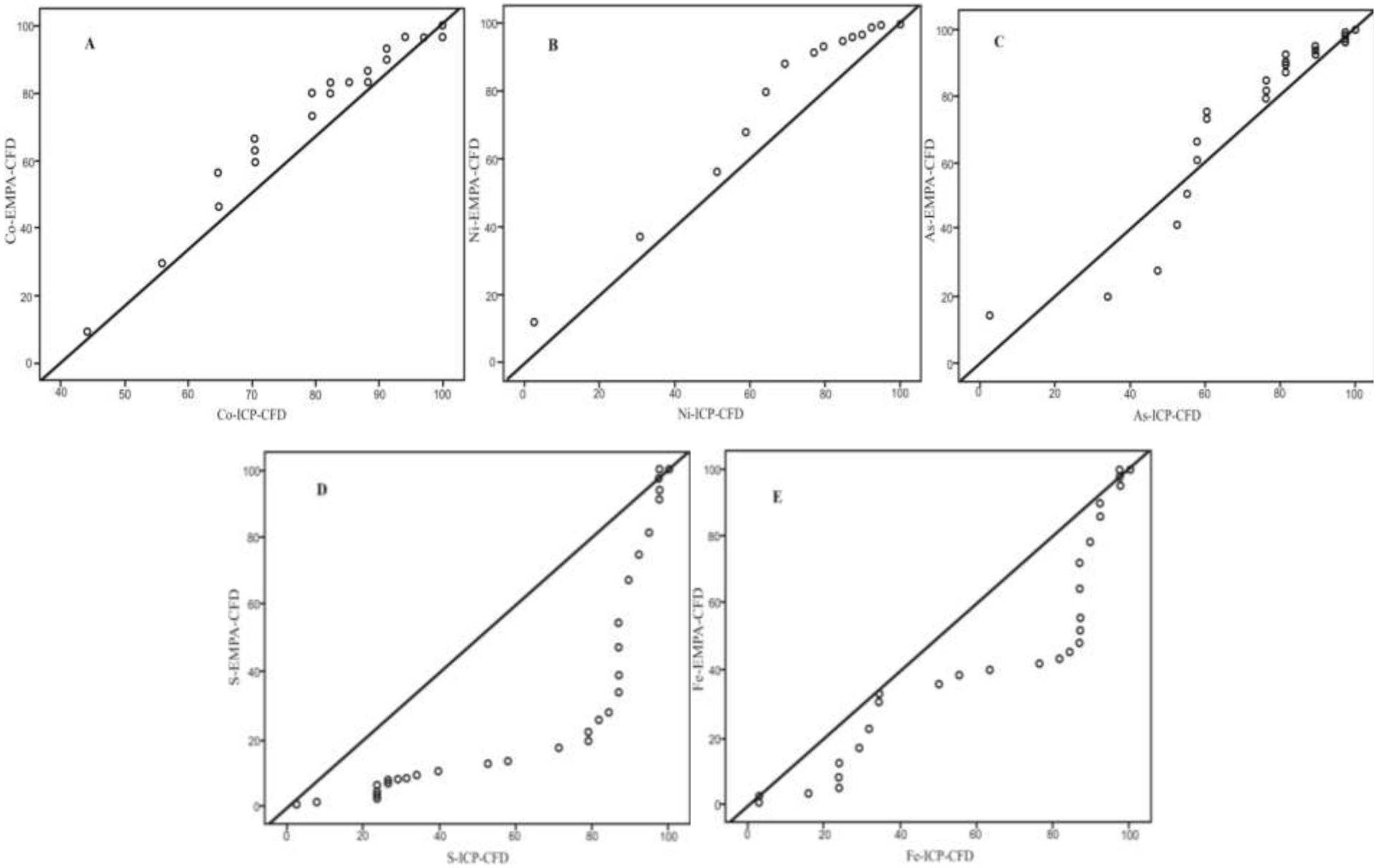

Figure 12A, B, C, D, and E. Cumulative frequency distribution (CFD) relation between EMP and raw LA-ICP-MS results, illustrating possible comparison between the two techniques especially of As, Co, and Ni.

Table 2. The maximum and minimum values of sulphur and iron isotopes (cps) in selected pyrite grains from Fairview, Sheba, and New Consort gold mines. It shows the large difference of isotopes in the same pyrite type and between the two pyrite types as mines well, which implies variations in the ablation rate rather that replacement effects.

Mine	Pyrite	^{33}S cps	^{34}S cps	^{56}Fe cps	^{57}Fe cps
Fairview	core-max	226244	1336544	196304000	4457994
Fairview	core-min	143640	858711	139736505	5683498
Fairview	rim-max	120634	750113	124248038	4786373
Fairview	rim-min	44081	270575	83339760	1978047
Sheba	core-max	209421	1270272	169724679	4133928
Sheba	core-min	102793	532756	138842500	3351508
Sheba	rim-max	255599	1385862	231599353	5233922
Sheba	rim-min	225381	451102	93026363	2540770
New Consort	core-max	98801	521850	137320700	3368286
New Consort	core-min	66542	398558	112879490	2591770
New Consort	rim-max	66307	1432455	264074753	6426195
New Consort	rim-min	65221	388756	3309647	3351600

and S (Figure 12 D and E), there are huge discrepancies such as differences in ablation rate, or/and pyrite's lattice defects. The box and whisker plots (Figure 10), and the comparison of the CFD for both techniques (Figure 12A, B, C, D, and E) show that, there are distinct overall similarities between the two datasets.

Isotopes relationships

Fractionation of isotopes using the raw LA-ICP-MS data

The raw LA-ICP-MS data of sulphur (^{33}S, ^{34}S) and iron isotopes (^{56}Fe, ^{57}Fe) from the Fairview Mine were examined to observe any differences in the isotope ratios and the possible relationship with the count per seconds (cps). The pyrite type 1 (cores) shows higher cps of both Fe and S isotopes compared to pyrite type 2 (rims) (Table 2). The isotopes values for the percentage abundance of normal distribution of S and Fe in the nature (De Laeter et al., 2003) were used to calculate the expected ratios of ^{34}S/^{33}S and ^{56}Fe/^{57}Fe. These values are ^{34}S: 4.25 (24), ^{33}S: 0.75(2), ^{56}Fe: 91.754(36), and ^{57}Fe: 2.119(10).

Based on the uncertainties in isotope abundance, a range (minimum and maximum) was defined, and then compared with the ^{34}S/^{33}S and ^{56}Fe/^{57}Fe ratios in pyrite from the Fairview Mine. Sheba and New Consort isotopes data were omitted because of insufficient information. Sulphur isotopes (^{33}S, ^{34}S) (cps) values in pyrite type1 (cores) (Table 2 and Figure 13A) vary by a factor of 2.5, and the values of these isotopes in pyrite type 1 (cores) are almost 5 times higher than in pyrite type 2 (rims). The ratio between ^{34}S and ^{33}S (Figure 13A) displays very slight scattering, which results in R_2 of 0.974 in pyrite type 1 (cores), and 0.996 in the pyrite type 2 (rims) from the Fairview Mine (N=26). The iron isotopes ^{56}Fe/^{57}Fe ratios (Figure 13B) show a distinct scatter within one pyrite type, and between the two different pyrite types (Figure 13B). The differences of iron isotopes (cps) between the pyrite types are close to 4 times at the Fairview Mine (Figure 13B). The iron isotopes in pyrite type 1 from the Fairview Mine are observed as 2 times higher than in pyrite type 2 from the same mine (Figure 13B). The ^{56}Fe/^{57}Fe ratios (Figure 13B) displays high scattering, which results in R_2 of 0.084 in pyrite type 1 (cores), and 0.947 in the pyrite type 2 (rims) from the Fairview Mine (N=26). This high scattering could be related to the intensive existence of mineral inclusions (pyrrhotite, chalcopyrite, etc.) inside pyrite type 1 (cores) more than pyrite type 2 (rims) which has lesser inclusions (Altigani et al., 2016).

Fractionation of sulphur and iron isotopes using the normalized isotopes to the SUM of LA-ICP-MS data

All the analysed isotopes were summed up and the total normalized. Even after normalizing, the sulphur isotopes in pyrite of the Fairview Mine vary widely (Figure 14A). The difference between sulphur isotopes of the two pyrite types is 3 times in the Fairview Mine. The iron isotopes (cps) vary by 3 times between the two types (cores and rims) of pyrite in the Fairview Mine (Figure 14B). However, the differences are very little compared when using the raw data. Normalising to the sum of all detected isotopes (cps), the differences between the high and low isotopes values is reduced to almost half, and the scattering of the values around the trend is condensed as well. The use of the sum of all counts of detected elements should be very similar (cps) for the different isotopes. However, the isotopes cps is still showing differences. The pyrite type 2 rims are also showing low

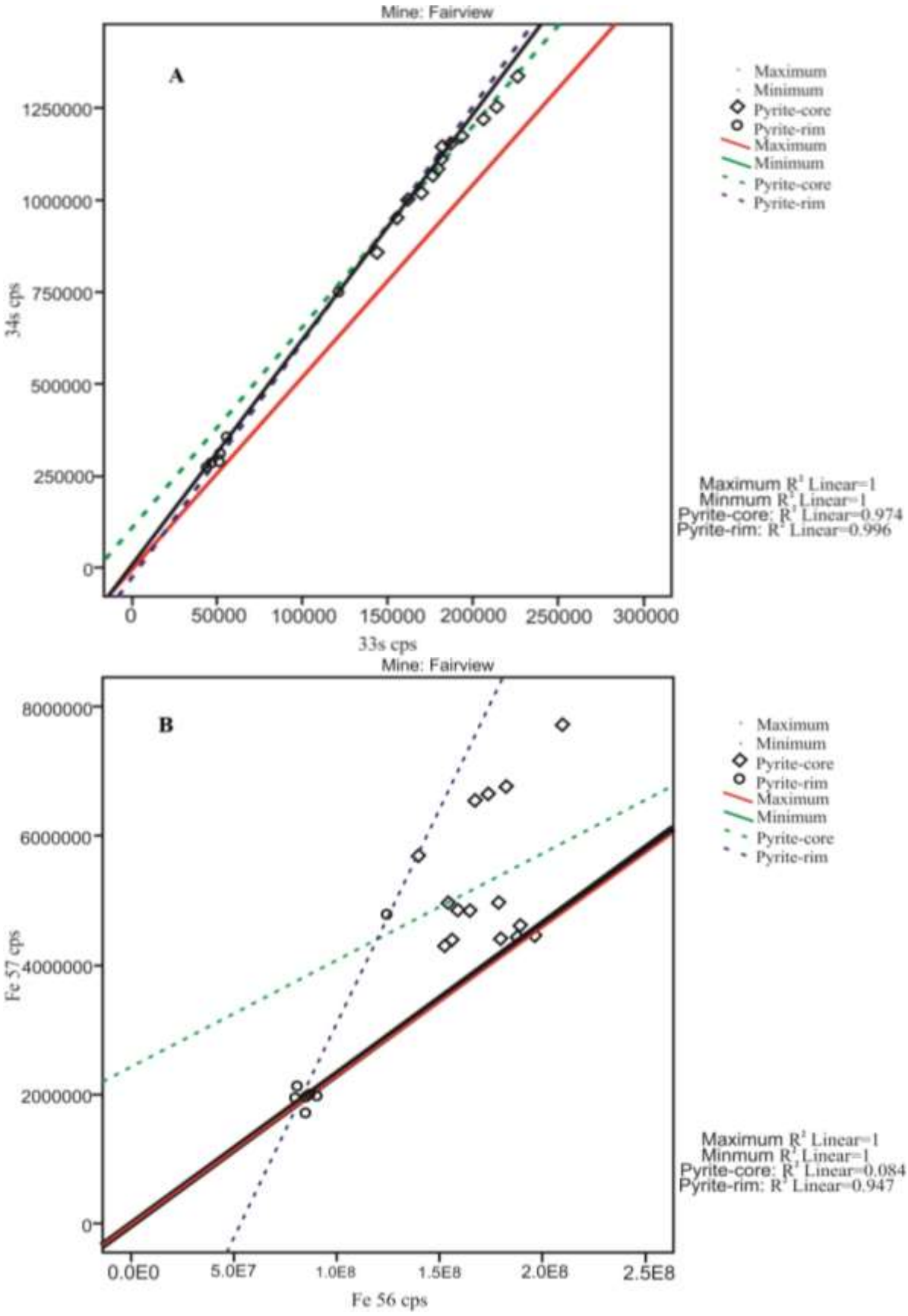

Figure 13. Sulphur and iron isotopes correlations in pyrite grains from the Fairview Mine, using raw LA-ICPMS data.

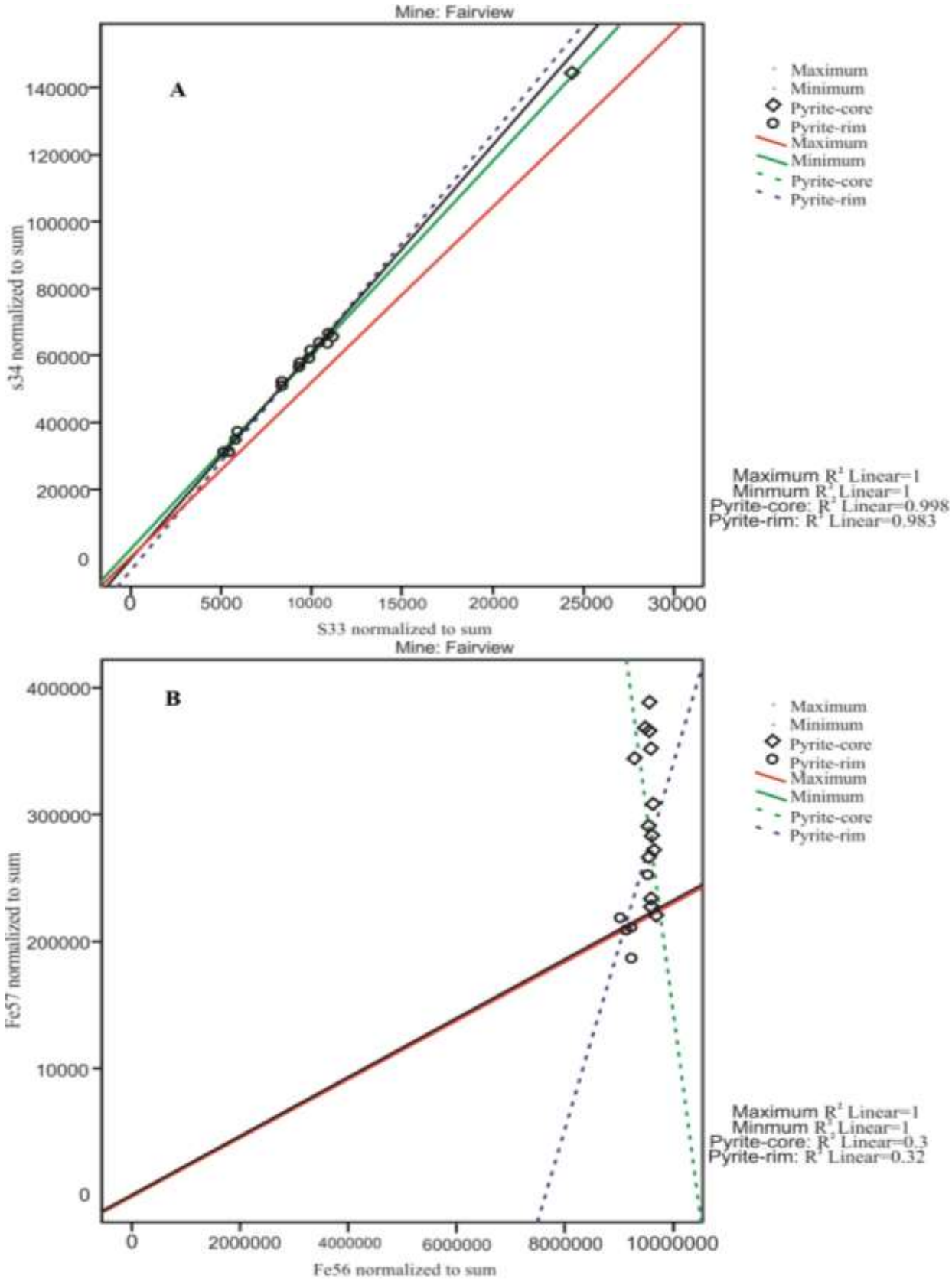

Figure 14. Relationships of sulphur and iron isotopes normalized to the sum of all counts per second in the Fairview Mine pyrite. It indicates no obvious fractionation; the variation of isotopes is due to less cps have been detected (variation in ablation rate).

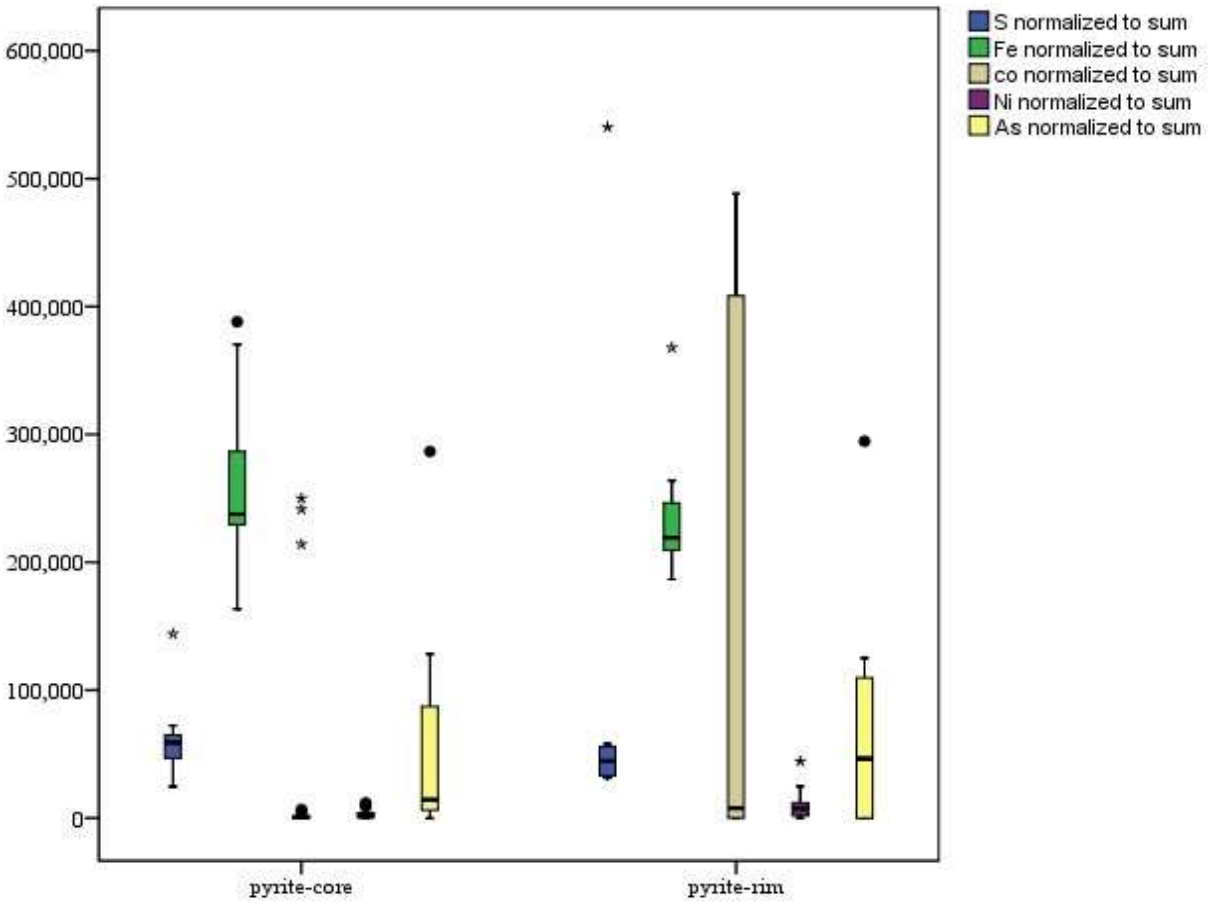

Figure 15. The differences in the major and trace elements in the pyrite type 1 and 2 from the Fairview Mine, which cusses the observed variations between the two pyrite types isotopes.

S and Fe raw data cps. The reason for this observation is seen in the As, Ni, and Co, which are minor elements in the pyrite of the Fairview Mine (Figure 15). The maximum value of iron isotopes in pyrite type 1 (cores) reduced from 8000000 cps to 400000 cps (almost 95 % reduction) after normalizing cps to all counts.

DISCUSSION

Non-systematic relationships between EMP and LA-ICP-MS results

Hypothetically, data obtained from the same pyrite grains, using the two different techniques should represent the same chemical composition, since they are applied to the same spots within the same pyrite grains. Several previous works used different standards to quantify LA-ICP-MS (cps) (Danyushevsky et al., 2011). This paper discusses the possible matching between the two methods applied on same pyrites. This study finds out there are lots of factors influencing the possibility to quantify cps based on wt. % results.

In order to avoid any unpredictable fluctuation in ablation rate due to intrinsic differences between pyrite grains, the data for each analysis were summed up, and normalized to the sum of the all reported isotopes. In this way, analytical errors, which can be caused by lower detection limits and the heterogeneity nature of the analysed grains, and inter-element fractionation, which might result from non-stoichiometric sampling during the ablation process, or incomplete vaporization of large particles (>125 nm) in the plasma, could be compensated for. Regardless of the all corrections in the (cps) values, usages of the raw (cps) data, sum of all counts, sulphur as internal standard, and iron as internal standard, no kind of any elemental relationships was observed between the results of the two techniques due to possible several factors, which are discussed next.

Spot size

The variations between the spatial resolution (analysed spots size) of the LA-ICPMS (~ 25 µm) and EMP (~ 4 µm) cause differences in the chemical results of the

examined pyrite grains (Figure 11). With the EMP method, the intergrowths, zoning and sub-micron inclusions (provided they are visible and spatially sufficiently separated) could easily be avoided during the analyses. In the LA-ICP-MS, the large analysed spot size causes analyses mixing in pyrite between the original composition (Fe_2S) and the inclusions and heterogeneities (likely Ni, As, Sb, and Co-richdomains), making it virtually impossible to compare the results. The spot size and depth are preferred to be fixed and constant during the analysis (Gaboardi and Humayun, 2009). Smaller spot size of analyses gives more precise results, due to smaller size of laser crater (EMP method), in which the analytical variation caused by zones and inclusions could be avoided. In addition, the use of lesser size of analysed material reduces the inter-elemental overlapping (Oriano et al., 2008). The sensitivity of the LAICP-MS machine depends on several factors: ablation efficiency, ionization efficiency, and ion transmission, which are controlled by spot size (Oriano et al., 2008). Moreover, the spot size influences the lower detection limit for the elements (Ciobanu et al., 2009).

Analysed volume (compositional variations)

For the LA-ICP-MS technique, the depth of ablation (~ 25 µm depth) is larger and represents more ablated material rather than the volume analysed by the EMP beam (~ 4 µm depth) (Figure 11). In addition to the unseen sub-surficial inclusions, the heterogeneity or zoned nature in most analysed pyrite grains (Altigani et al., 2016) challenges the comparison between the two techniques (Cook et al., 2009a), and subsequently standardization. The amount of material ablated varies with minor differences in chemical composition (all are pyrite grains). Moreover, substitutions and replacement processes between major and trace elements, which were observed quite often in the selected pyrite grains that produced notably variation in ablation rate. Although, ablating more material gives the possibility to smooth out the effects of inclusions and reach low detection limits which is recommended (Li and Audétat, 2012). However, these inclusion results can destroy the overall elemental relationships within pyrite (Cook et al., 2009b). Besides that, the existence of sub-microscopic inclusions and heterogeneous nature of analysed pyrite upsurges the inter-elemental fractionation during ablation (Deditius et al., 2011).

Isotopes fractionation

This research also aims to identify any ablation effects on the values or ratios of the sulphur and iron isotopes (the main constituents in pyrite lattice structure). Differences were observed in both sulphur and iron values of the studied pyrite types (cores and rims). Generally, the variation in isotope values between different pyrite types reflects genetic processes, and possibly thermo-chemical sulphate reduction during the early sulphide formation (Johnston, 2011; Bühn et al., 2012). The variation between sulphur isotopes values in pyrite is due to the differences in formation temperatures or oxidation and reduction reactions. These oxidation and reduction reactions commonly occur at: (1) high temperatures in the igneous systems, (2) intermediate temperatures in the hydrothermal systems, and (3) low temperatures in the sedimentary (organic) system (Seal, 2006). The fluctuation in sulphur and iron isotopes values is also indicative of change in the chemistry of the ores (Hill et al., 2010).

The dominant ^{32}S isotope was not used in this research due to its huge interference with oxygen ($^{16}O_2$) during ablation; therefore ^{33}S and ^{34}S were reported to evaluate the differences in counts per seconds. Obviously, increase of ^{34}S and ^{33}S in the pyrite reflects decrease in the detected ^{32}S values and vice versa. This does not imply fractionation between these isotopes; it is due to differences in ablation rates. Most of the sulphur and iron isotope ratios in the studied pyrite grains of the Fairview Mine are within the max-min range, which indicates no detectable fractionation processes have affected pyrite of this mine. However, the observed large-scale scattering between the iron isotopes (^{56}Fe and ^{57}Fe) in the different pyrite types is probably due to the interference of ^{40}Ar and $^{16}O_2$ with ^{56}Fe or to lesser degree with ^{57}Fe (Danyushevsky et al., 2011). The cps values of both $^{34}S/^{33}S$ and $^{56}Fe/^{57}Fe$ isotopes are higher ablation rate in the older type of pyrite (core), which is heterogeneous and contains more inclusions (cause lattice defects) compared to the younger type of pyrite (rims) (Altigani et. al., 2016). This is inconsistent with the observations of Yoshiya et al. (2012), who noticed an increase of ^{56}Fe cps values with euhedral morphology of the pyrite, and it decreases with irregular pyrite shapes. That also reflects possible effects of deformation in pyrite crystal lattice on the ablation rate, and consequently in the detected concentration (cps) values. Nevertheless, the LA-ICP-MS instrument technology used in this research is not suitable for such justifications.

Although, both pyrite types in the Fairview Mine are subjected (with different intensity) to replacement processes, metasomatism, and uncertain chemical relationships. The variations in the isotopes (cps) are too large to relate them to elemental substitutions, fractionation, or redox processes. If sulphur and iron as major identifiable elements in the pyrite were replaced by As, or (Ni + Co) respectively; by factor up to 6 then analysed grains would have to present totally different minerals. The normalized data to the sum of all determined isotopes show better sulphur isotopes relationship than using the raw data. However, even after normalizing the counts, huge variations in counts were

observed in all pyrite types. Small variations in minor elements would make huge variations in the ablation rate. In the relationships between elements in pyrite using LA-ICP-MS, it was noticed that slight substitutions should make huge variations in the ablation rates, and subsequently affect the output of concentrations (cps) for a certain element.

Conclusions

LA-ICP-MS data of the three studied mines were reported in count per seconds (cps), while EMP results were counted as weight percentage (wt. %). In this research, standardization of the LA-ICP-MS data was based on the EMP results obtained from the same analysed spots; however, no direct relationships were observed. Several procedures were used in this research to quantify the LA-ICP-MS result, based on specific isotopes of sulphur, and iron as internal standards. Normalization to the total of all counts is also used in this term. However, none of these attempts were working out. The discrepancies are caused by variations in ablation rates between certain elements (Fe - Ni or S - As), differences in spot depths and sizes, and variation in accuracy and limits of detection in both techniques.

The comparative statistical methods show that the data obtained by EMP and LA-ICP-MS are log-normally distributed; it also suggests to some extent, that there are similarity patterns of the two techniques distribution. However, these similarities are not reflecting any kind of direct or linear (systematic) relationships. It is believed to be caused by one or more of these factors: (a) the differences in the ablation rate during the LA-ICP-MS machine running, (b) the instrumental problems, (c) variations in spot size and depths used in both techniques, (d) inclusions effect, and (e) probably the sensitivity and limits of detection for the two techniques.

CONFLICT OF INTERESTS

The author has not declared any conflict of interests.

ACKNOWLEDGEMENTS

The author appreciates the input of the staff at the Geology Department of the University of Pretoria, the South African Forensic Laboratory in Pretoria, and Alneelain University in Sudan who sponsored the research leading to this contribution. The encouragement of Napoleon Hammond is greatly appreciated. An early version of this manuscript was much improved through the exceptionally insightful comments of Prof. RKW Merkle.

REFERENCES

Altigani MAH, Merkle RKW, Dixon RD (2016). Geochemical identification of episodes of gold mineralisation in the Barberton Greenstone Belt, South Africa. Ore Geology Reviews 75:186-205.

Bi S, Li J, Zhou M, Zhan L (2011). Gold distribution in As-deficient pyrite and telluride mineralogy of the Yangzhaiyu gold deposit, Xiaoqinling district, southern North China Craton, Mineral Deposita 46:925-941.

Bühn B, Santos RV, Dardenne MA, de Oliveira CG (2012). Mass-dependent and mass-independent sulfur isotope fractionation ($\delta^{34}S$ and $\delta^{33}S$) from Brazilian Archean and Proterozoic sulfide deposits by laser ablation multi-collector ICP-MS, Chemical Geology, pp. 312-313:163-176.

Ciobanu CL, Cook NJ, Pring A, Brugger J, Danyushevsky LV, Shimizu M (2009). 'Invisible gold' in bismuth chalcogenides. Geochimica et Cosmochimica Acta 73:1970-1999.

Chen Z (1999). Inter-element fractionation and correction in laser ablation inductively coupled plasma mass spectrometry. Journal of Analytical Atomic Spectrometry 14:1823-1828.

Cook NJ, Ciobanu CL, Mao J (2009a). Textural control on gold distribution in As-free pyrite from the Dongping, Huangtuliang and Hougou gold deposits, North China Craton. Chemical Geology 264:101-121.

Cook NJ, Ciobanu CL, Pring A, Skinner W, Shimizu M, Danyushevsky L, Saini-Eidukat B, Melcher F (2009b). Trace and minor elements in sphalerite: A LA-ICP-MS study. Geochimica et Cosmochimica Acta 73:4761-4791.

Cook NJ, Ciobanu CL, Danyushevsky LV, Gilbert S (2011). Minor elements in bornite and associated Cu-(Fe)-sulfides: A LA-ICPMS study. Geochimica et Cosmochimica Acta 73:4761-4791.

Danyushevsky L, Robinson P, Gilbert S, Norman M, Large S, McGoldrick P, Shelley S (2011). Routine quantitative multi-element analysis of sulphide minerals by laser ablation ICP-MS: Standard development and consideration of matrix effects, Geochemistry: Exploration, Environment, Analysis 11:51-60.

De Laeter JR, Böhlke JK, De Bièvre P, Hidaka H, Peiser HS, Rosman KJR, Taylor PDP (2003). Atomic weights of the elements: Review 2000 (IUPAC Technical Report). Pure Applied Chemistry 75(6):683-800.

Deditius AP, Utsunomiya S, Reich M, Kesler SE, Ewing RC, Hough, R, Walshe J (2011). Trace metal nanoparticles in pyrite. Ore Geology Reviews 42:32-46.

Gaboardi M, Humayun M (2009). Elemental fractionation during LA-ICP-MS analysis of silicate glasses: implications for matrix-independent standardization. Journal of Analytical Atomic Spectrometry 24:1188-1197.

Godel B, Barnes SJ (2008). Platinum-group elements in sulfide minerals and the whole rocks of the J-M Reef (Stillwater Complex): Implication for the formation of the reef. Chemical Geology 248:272-294.

Halter WE, Pettke T,Heinrich CA (2004). Laser-ablation ICP–MS analysis of silicate and sulfide melt inclusions in an andesitic complex I: analytical approach and data evaluation. Contributions to Mineralogy and Petrology 147:385-396.

Heinrich CA, Pettke T, Halter WE, Aigner-Torres M, Audetat A, Gunther D, Hattendorf B, Bleiner D, Guillong M, Horn I (2003). Quantitative multi-element analysis of minerals, fluid and melt inclusions by laser-ablation inductively-coupled-plasma mass-spectrometry, Geochimica et Cosmochimica Acta 67(18):3473-3496.

Hill PS, Schauble EA,Young ED (2010). Effects of changing solution chemistry on Fe^{3+}/ Fe^{2+} isotope fractionation in aqueous Fe-Cl solutions, Geochimica et Cosmochimica Acta 74:6669-6689.

Humayun M, Davis FA, Hirschmann MM (2010). Major element analysis of natural silicates by laser ablation ICP-MS. Journal of Analytical Atomic Spectrometry 25:998-1005.

Johnston DT (2011). Multiple sulfur isotopes and the evolution of Earth's surface sulphur cycle. Earth-Science Reviews 106:161-183.

Li Y, Audétat A (2012). Partitioning of V, Mn, Co, Ni, Cu, Zn, As, Mo, Ag, Sn, Sb, W, Au, Pb, and Bi between sulfide phases and hydrous basanite melt at upper mantle conditions. Earth and Planetary Science Letters 355:327-340.

Oriano CD, Da Pelo S, Podda F, Cioni R (2008). Laser-Ablation Inductively Coupled Plasma Mass Spectrometry (LA-ICP-MS):

Setting operating conditions and instrumental performance, Periodico di Mineralogica 77:65-74.
Seal RR (2006). Sulfur Isotope Geochemistry of Sulfide Minerals. Reviews in Mineralogy and Geochemistry 61:633-677.
Shaheen ME, Gagnon JE, Fryer BJ (2012). Femtosecond (fs) lasers coupled with modern ICPMS instruments provide new and improved potential for in situ elemental and isotopic analyses in the geosciences. Chemical Geology (330-331): 260-273.
Sylvester PJ, Cabri LJ, Tubrett MN, McMahon G, Laflamme JHG, Peregoedova A (2005). Synthesis and evaluation of a fused pyrrhotite standard reference material for platinum group element and gold analysis by laser ablation-ICPMS, in Törmänen TO, Alapieti TT, eds., 10th International Platinum Symposium 2005, Oulu, Geological Survey of Finland, Extended Abstracts 16-20.
Sylvester PJ. (ed.) (2008). Laser ablation-ICP-MS in the earth sciences: Current practices and outstanding issues. Mineralogical Association of Canada, Short Course, 348p.
Thomas R (2004). Practical Guide to ICP-MS. Marcel Dekker Inc. New York, USA 393p.
Watling RJ, Herbert HK (1994). Gold fingerprinting by laser ablation inductively coupled plasma mass spectrometry, Spectrochimica Acta Part B: Atomic Spectroscopy 499(2):205-219.
Winderbaum L, Ciobanu CL, Cook NJ, Paul M, Metcalfe A, Gilbert S (2012). Multivariate Analysis of an LA-ICP-MS Trace Element Dataset for Pyrite: International Association for Mathematical Geosciences 44:823-842.
Woodhead J, Hergt J, Meffre S, Large RR, Danyushevsky D, Gilbert S (2009). In situ Pb-isotope analysis of pyrite by laser ablation (multi-collector and quadrupole) ICPMS. Chemical Geology 262:344–354.
Yoshiya K, Nishizawac M, Sawakia Y, Uenoa Y, Komiyab T, Yamadae K, Yoshidab N, Hirataf T, Wadag H, Maruyamaa S (2012). In situ iron isotope analyses of pyrite and organic carbon isotope ratios in the Fortescue Group: Metabolic variations of a Late Archean ecosystem. Precambrian Research 212-213:169-193.
Yuan JH, Zhan XC, Fan CZ, Zhao LH, Sun DY, Jia ZR, Hu MY, Kuai LJ (2012). Quantitative analysis of sulfide minerals by laser ablation-inductively coupled plasma-mass spectrometry using glass reference materials with matrix normalization plus sulfur internal standardization calibration, Chinese Journal of Analytical Chemistry 40(2):201-207.